Article:
FELL, HENRY (2026) Integrating microclimate to understand vector development and disease patterns: challenges and lessons from plague in Madagascar's Central Highlands. Proceedings of the Royal Society B: Biological Sciences. 20252496. ISSN: 1471-2954

https://doi.org/10.1098/rspb.2025.2496

PROCEEDINGS B

royalsocietypublishing.org/journal/rspb

Research

Cite this article: Fell HG *et al*. 2026 Integrating microclimate to understand vector development and disease patterns: challenges and lessons from plague in Madagascar's Central Highlands. *Proc. R. Soc. B* **293**: 20252496.
https://doi.org/10.1098/rspb.2025.2496

Received: 29 September 2025
Accepted: 9 February 2026

Subject Category:
Ecology

Subject Areas:
ecology, health and disease and epidemiology

Keywords:
plague, *Yersinia pestis*, microclimate, null modelling, zoonotic disease

Author for correspondence:
Henry Gillies Fell
e-mail: hgfell@gmail.com

Integrating microclimate to understand vector development and disease patterns: challenges and lessons from plague in Madagascar's Central Highlands

Henry Gillies Fell[1,3], Joseph Bailey[4], Fanohinjanaharinirina Rasoamalala[5,6], Beza Ramasindrazana[5], Luke Shipley[2], Matthew Jones[1], Voahangy Andrianaivoarimanana[2], Katharina Kreppel[7], Nils Christian Stenseth[8,9,10], Ilya M. D. Maclean[11], Minoarisoa Rajerison[5], Adam C. Algar[12,†] and Steve Atkinson[2,†]

[1]School of Geography, and [2]Biodiscovery Institute, University of Nottingham, Nottingham, UK
[3]BioArCh, Department of Archaeology, University of York, York, UK
[4]Department of Biology, Anglia Ruskin University—Cambridge Campus, Cambridge, UK
[5]Plague Unit, Institut Pasteur de Madagascar, Antananarivo, Madagascar
[6]Faculty of Sciences, University of Antananarivo, Antananarivo, Madagascar
[7]Department of Public Health, Institute of Tropical Medicine, Antwerp, Flanders, Belgium
[8]The Centre for Pandemics and One-Health Research, Sustainable Health Unit, Institute of Health and Society, Faculty of Medicine, and [9]Centre for Ecological and Evolutionary Synthesis (CEES), Faculty of Mathematics and Natural Sciences, University of Oslo, Oslo, Norway
[10]Vanke School of Public Health, Tsinghua University, Beijing, People's Republic of China
[11]Environment and Sustainability Institute, University of Exeter, Exeter, UK
[12]Department of Biology, Lakehead University, Ontario, Canada

HGF, 0000-0001-6009-4270; LS, 0000-0003-1521-8670; MJ, 0000-0001-8116-5568; NCS, 0000-0002-1591-5399; IMDM, 0000-0001-8030-9136; ACA, 0000-0001-8095-0097

Plague, the zoonotic vector-borne disease caused by the bacterium *Yersinia pestis*, shows seasonal infection patterns across the Central Highlands of Madagascar. The disease persists within a complex ecological network involving host and vector species, all influenced by climate. Due to this complexity, links between climate, *Y. pestis* ecology and human infection remain incomplete. This study developed microclimate-based models to assess climatic impacts on growth cycles of plague vectors *Xenopsylla cheopis* and *Synopsyllus fonquerniei*. Using microclimatic modelling, the vector development index (VDI) was calculated to estimate annual developmental phases for each flea species. The uncorrected VDI suggested that development rates were highly variable for *X. cheopis* compared to *S. fonquerniei*, which shows greater temporal consistency. Elevated VDI slopes, representing an increased rate of vector development, correlated with plague cases across 61.8–14.7% of areas, implying possible climatic influence on vector-driven disease cycles. However, these associations were not maintained after adjusting modelled temperatures using limited field validation. These findings highlight the complex interactions between climate, vector dynamics and *Y. pestis* transmission, and emphasize the need for further investigation into burrow microclimates and their seasonal epidemiological roles.

1. Introduction

Yersinia pestis, the bacterium that causes the acute febrile disease known as plague, occupies a prominent place in human history, having claimed tens of millions of lives through periodic pandemics, and is arguably the

[†]Joint final authors.

Electronic supplementary material is available online at https://doi.org/10.6084/m9.figshare.c.8335608.

THE ROYAL SOCIETY PUBLISHING

most dangerous bacterial pathogen that humans have ever had to face. In 2006, the World Health Organization (WHO) classified *Y. pestis* as a re-emergent pathogen primarily due to an increase in infection rates across Africa [1,2]. Madagascar records the highest annual number of human plague cases globally [3] with a permanent reservoir cycling between human and wildlife populations [4,5]. Seasonal outbreaks and high fatality rates highlight the susceptibility of vulnerable groups of the Madagascan population to the disease [6]. When considered in the context of the speed of transmission, high level of virulence and extremely rapid time to death, the importance of understanding factors that may facilitate the zoonotic transmission of *Y. pestis* from wildlife reservoirs to human populations is paramount.

Wildlife reservoirs and human populations in the rural areas of the Central Madagascan Highlands experience seasonal fluctuations in *Y. pestis* infections [7,8] above 800 m above sea level, with further cases occasionally reported in the north and on the west coast of the island [9,10]. Human plague cases normally occur during the warm and rainy season from September to March, although in recent years, cases have been reported in August [11]. The beginning of the plague season is thought to follow a period of low host species abundance and coincides with high abundance of adult fleas of the endemic species *Synopsyllus fonquerniei* [7,11–13].

The geographical isolation of the disease in the Central Highlands is probably due to the infection and transmission of specific host and vector species. The timing of vector development is thought to be pivotal to the timing of the plague season, as bubonic plague infections are caused by a *Y. pestis*-infected flea bite. The black rat (*Rattus rattus*) is considered the primary host, although other species such as the brown rat (*Rattus norvegicus*) and the Asian shrew (*Suncus murinus*), as well as endemic species such as the forest-dwelling Tenrecinae subfamily, have also tested seropositive for *Y. pestis* [14–16]. A range of flea species parasitize these hosts, but *Xenopsylla cheopis* and *S. fonquerniei* are those most commonly found to be infected with *Y. pestis* and hence considered key to the maintenance of *Y. pestis* [4,7,9,10,16]. The primary vector of *Y. pestis* globally is *X. cheopis*, while *S. fonquerniei* is endemic to Madagascar [9,10,17]. Due to its temperature tolerances, *S. fonquerniei* is confined to the Central Highlands and may be an important factor in limiting the spread of *Y. pestis* beyond the endemic regions [9].

Climate may influence the incidence of *Y. pestis* infections in humans and host species globally [18,19], and in Madagascar, human plague incidence is correlated with regional climate drivers such as El Niño–Southern Oscillation and Indian Ocean Dipole [12]. However, host and vector species in their micro-habitats do not experience broad-scale climate phenomena directly but through micro-habitats that may differ from the broader macroclimate [20]. Developmental rates of *S. fonquerniei* and *X. cheopis* depend on temperature and humidity, thus the conditions to which these species are exposed in the wild could predict their respective population dynamics [21]. Both species' pre-imaginal development occurs in rodent burrows, which are somewhat protected from changes in ambient temperatures [22]. The temperature of a burrow is a depth-dependent weighting of above-ground temperature and soil temperatures [23]. In the Central Highlands, burrow temperature and humidity vary throughout the dry and wet seasons (17–22°C, 65–81% and 23–28°C, 84–94%, respectively) [24], while burrows within human dwellings, which are preferred by *X. cheopis*, are generally found to be warmer and dryer with less variation; this coincides with a limited seasonal variation *of X. cheopis* abundance [25,26]. This suggests that the population dynamics of this species may not impact the timing of human plague seasonality [7]. In contrast, the maximum abundance of *S. fonquerniei* is observed in October/September, after a prolonged period of development throughout the cooler dry season (May–September) when both humidity and burrow temperature are low [25]. As such, this maximum abundance coincides with the beginning of the human plague infection season in the Central Highlands [7]. Together, these patterns suggest that both the distribution and the seasonality of human plague infection in Madagascar may be strongly dependent on the temperature and humidity sensitivity of *S. fonquerniei*.

The dynamics of host and vector species and microclimate in combination mediate the seasonal fluctuation of *Y. pestis* infections across Madagascar [5]. Thus, understanding the mechanisms that link the abiotic variables, the dynamics of all these species, and *Y. pestis* is key to understanding the spatio-temporal distribution of plague across Madagascar. However, the complexity of the plague–climate nexus has made it difficult to identify the mechanisms that contribute to observed climate and plague correlations [12,27], and relying on macroclimate models to predict microclimate is limited as they operate at higher spatio-temporal scale and fail to account for subtle variations such as ground temperatures below seasonal vegetation [28]. Fortunately, microclimates can be surveyed using localized climatic monitoring and modelling [29–31] and then used in vector disease studies that enable predictions of vector population dynamics that reflect biologically relevant microclimatic conditions [21,32].

Here, we model spatio-temporal rates of plague vector development as a function of microclimate variation across the Central Highlands from 2014 to 2020. We then test the hypothesized relationship between vector development, particularly of *S. fonquerniei*, and human plague infection by determining whether the timing and location of human plague cases have been more likely to occur when conditions have been favourable for vector development.

2. Methods

(a) Study area

We focus on the Central Highlands of Madagascar (approx. 170 000 km^2, figure 1) and consider two administration levels: districts and communes. Microclimate data were obtained from the Ambositra, Antsirabe and Ankazobe districts and weather station data from Ankazobe and Antananarivo. Human plague case data included information from across Madagascar, which we subset to include only data from the Central Highlands.

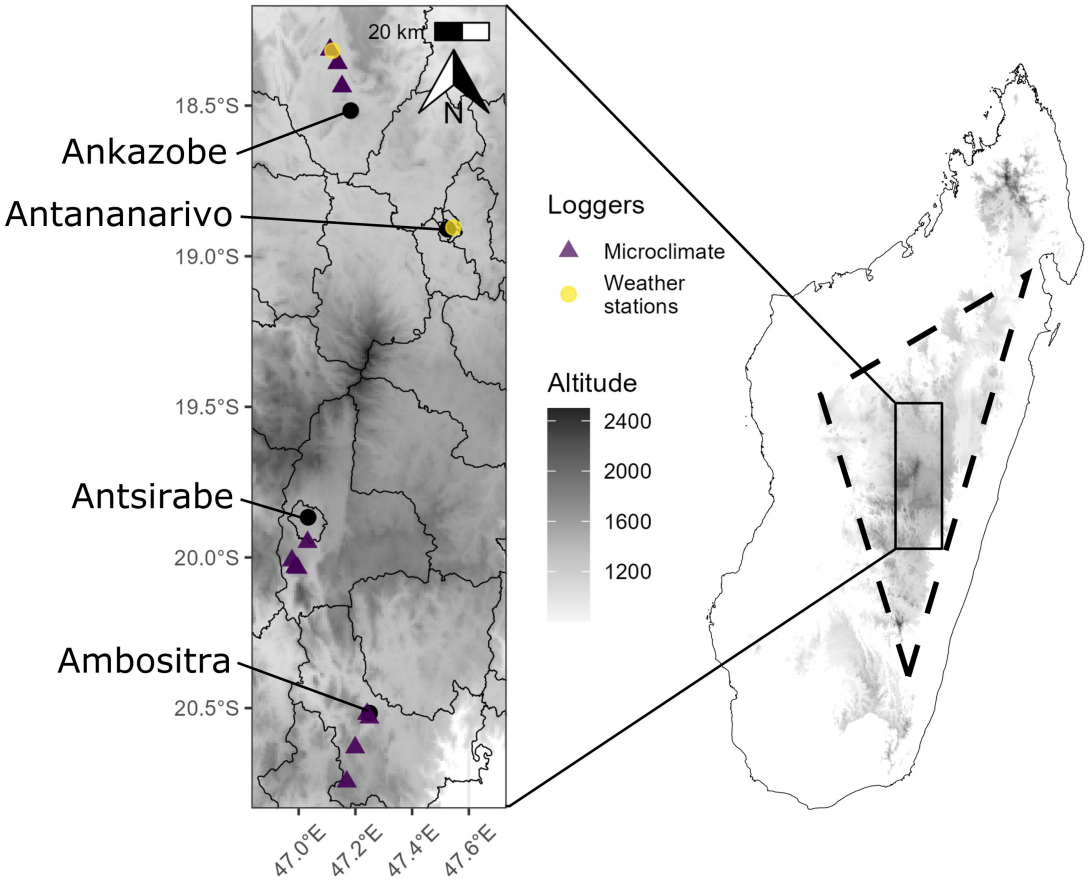

Figure 1. The Central Highlands of Madagascar, and the area of data validation. Grey shading is used to show altitudes above 800 m; the dashed line denotes the Central Highlands. The expanded area of interest map shows key cities, district boundaries and locations of micro- and macroclimatic validation.

(b) Microclimate modelling and validation

The open-source mechanistic microclimate model *microclimf* (https://github.com/ilyamaclean/microclimf) was used to model the below-ground temperature at a depth of 15 cm to represent burrows inhabited by *R. rattus*. *microclimf* is part of a suite of microclimate modelling packages including *microclima* [31] and *microclimc* [33], with functionality shared across all 3. microclimf was developed specifically for computational efficiency across large spatial extents while further refining the method used for quantifying heat and vapour transfer below the canopy [34].

Meteorological and environmental data, including temperature, humidity, precipitation, land cover and soil texture classification, were used as inputs for the *microclimf* model (figure 2). These data were derived from ERA5 climate reanalysis, MODIS land cover and iSDA soil databases, ensuring compatibility with the model's requirements through specific transformations [35–37] (electronic supplementary material, text S1). Validation of the macroclimatic data was conducted with field measurements from two weather stations, recording data at a 15 min resolution since installation (July 2023 to present). Microclimate measurements were recorded from 15 sites across the Central Highlands using a combination of TOMST TMS-4 loggers and Easy Log data loggers (EL USB-2, Lascar Electronics) at a resolution of 15 and 30 min, respectively, across 24 h data collection periods at each site (figure 1; electronic supplementary material, text S2 and figure S1).

(c) Modelling vector development

We used methods adapted from Kafle *et al.* [38] to transform the microclimatic model to a temporal model of vector development, which we refer to as the vector development index (VDI). This VDI represents the count of pre-imaginal (larval and pupal) development cycles a vector could complete within a set amount of time, given the climatic conditions to which it was exposed, all else being equal. Although mortality decreased at higher temperatures in both species, we did not attempt to include the impact of temperature on mortality rate, as it was only calculable during the larval growth phase, as death day could not be accurately determined for pupae [24]. Furthermore, Kreppel [25] highlights how climatic effects on mortality differ between field and laboratory conditions, cautioning against overinterpreting these findings. The slope of the VDI, therefore, represents a proxy for development rate. This vector development model was subsequently analysed against the timing of human plague cases across the Central Highlands to investigate if there could be a causal link (figure 2).

Modelled temperature at a depth of 15 cm below the ground surface (−0.15 m) was used as an input variable to a further mechanistic model to determine the number of pre-imaginal (larval and pupal) development cycles a vector could complete in 1 year in each grid cell (VDI) [38]. We initially calculated annual degree days (ADD) for each vector species. ADD were calculated as the sum of the daily temperatures in a year when the mean daily temperature (derived from the hourly below-ground

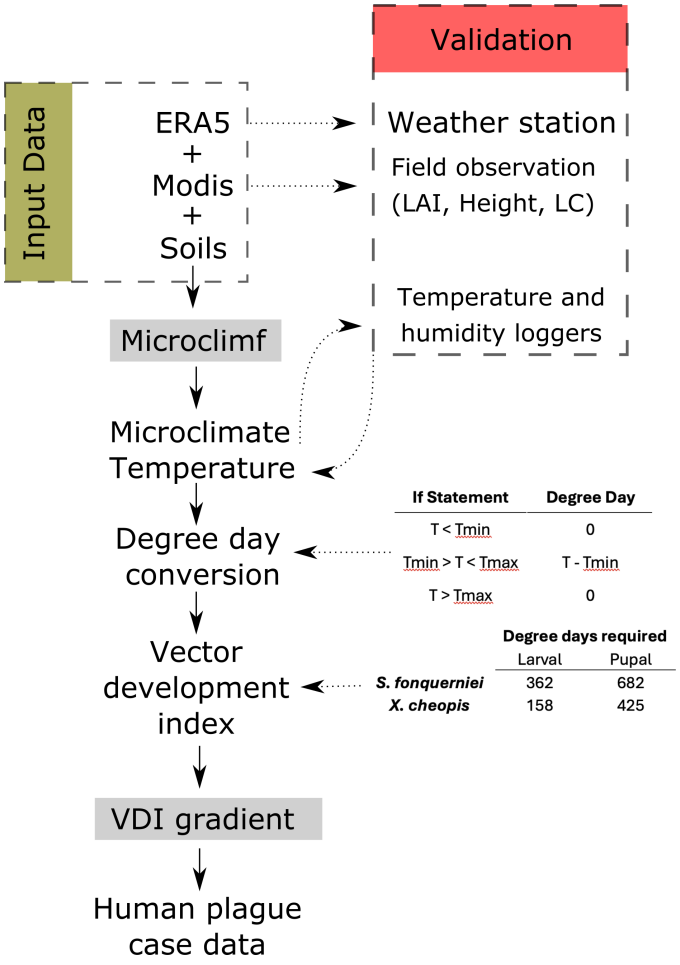

Figure 2. Data processing pathway. Illustrating analysis from the initial input and validation of land cover data through to microclimate model creation. This was followed by microclimatic validation and correction. The microclimate model was then converted to degree-day data and subsequently transformed into a spatial representation of the VDI for each species. A VDI slope (vector development rate) was then calculated and finally compared to the occurrence of human plague cases across the Central Highlands of Madagascar.

temperature data) was within the temperature development range of each species [38]. The lower development limit was 9°C and 12.5°C for *S. fonquerniei* and *X. cheopis*, respectively [24,39]. The upper limit for *X. cheopis* was 36.5°C [26]. As the upper developmental limit *S. fonquerniei* has not, to our knowledge, been determined, we also used 36.5°C for this, which may not account for the observed cold adaptation of *S. fonquerniei* [24,26]. ADD were not determined for days where the mean daily temperature was outside the development range. *K*-values for each species were then calculated as the sum of degree-days required for 50% of the population to complete their pre-imaginal growth stages (682 for *S. fonquerniei* and 425 for *X. cheopis*). *K* was estimated as the reciprocal of the slope of a linear regression of development time against temperature [24]. These data were then combined cumulatively across the period of investigation. To compute the VDI, the ADD was then divided by each species's *K*-value.

(d) Human plague data

We used positive reported human plague cases from across the Central Highlands from 2014 to 2020 at two administrative resolutions. The data at the second administrative level (districts) cover the 2014–2020 time window, and the data at the third administrative level (communes) cover the 2018–2020 time window. The human plague case data from 2014 to 2020 were gathered from notifications of suspected plague cases to the Central Laboratory for Plague of the Malagasy Ministry of Health, housed within the Plague Unit of the Institut Pasteur de Madagascar. From these data, only confirmed plague cases, as defined by the WHO plague case definitions, were included in the analysis [40]. Only bubonic plague cases were used, as they result from an infected flea bite and are therefore likely to be representative of the *Y. pestis–vector*–transmission cycle. There was a small discrepancy in bubonic case reporting between the district and the commune administrative levels.

(e) Prediction of human plague using vector development index

We tested the hypothesized link between climate, vector development and human plague cases by assessing whether the rate of vector development (slope of VDI vs time) in each area prior to human plague cases was greater than expected if human plague cases occurred randomly. At each human plague case location, we calculated the VDI slope prior to each case for a range of potentially biologically relevant periods (1, 2, 3 and 6 months), based on the lifespan of adult *X. cheopis* of between 2 and 9

months, as the lifespan of *S. fonquerniei* was not specified in the literature [41]. The slope was determined as the coefficient of a linear model of mean VDI against time for the 1, 2, 3 and 6 month windows prior to the recorded cases. We then compared the extracted slopes to null slopes. These null slopes were generated by randomly moving the date of the recorded cases in each area while maintaining the temporal structuring of the cases across that area within the sampling windows (2014–2020 and 2018–2020). The null slopes were then calculated by extracting the slopes prior to these null human plague cases, and this process was repeated 1000 times per area. We then determined whether the recorded VDI slopes were significantly greater than the null values, which, if confirmed, would suggest that climatically mediated vector development contributes to initial plague infection in humans. To determine whether the recorded VDI slopes were significantly greater than the nulls, *p*-values were calculated directly following eqn 1 in Ruxton *et al.* [42].

3. Results

(a) Climatic data validation

The ERA5 data showed a high agreement with weather station data for Ankazobe and Antananarivo, with Spearman correlation coefficients of 0.941 and 0.929, respectively, and RMSE values below 2°C for both locations (electronic supplementary material, figure S2). However, the microclimate model underpredicted both above- and below-ground temperatures, with the largest discrepancies observed below ground (electronic supplementary material, figure S3). There may be a precedent for the TOMST TMS-4 loggers over-reading temperature at near and below surface height, which may contribute to the observed model underprediction; however, this underprediction was observed using both the TOMST TMS-4 and Easy Log data loggers (electronic supplementary material, text S3) [43]. To account for this possible bias, we performed subsequent analyses using the modelled burrow temperatures before and after applying a temperature correction. The temperature correction, which we applied to the −0.15 m modelled temperatures, was +6.03°C, which was the mean difference between the modelled and measured temperatures at −0.15 m depth (electronic supplementary material, text S3, figures S2 and S3). The results are presented using the uncorrected and corrected temperatures throughout.

(b) Vector development index comparison between species and areas

Consistently across administrative areas and temperature correction methodology, *X. cheopis* had a higher mean VDI than *S. fonquerniei* (figure 3). The difference in mean VDI was relatively small across the uncorrected temperatures with mean values of 7.215 (min = 4.499, max = 9.119) and 9.232 (min = 4.999, max = 14.342) at the district level and 7.344 (min = 5.553, max = 9.141) and 9.423 (min = 6.530, max = 14.568) at the commune level for *S. fonquerniei* and *X. cheopis*, respectively. This difference in mean VDI was much higher for corrected microclimatic temperatures with means of 10.882 (min = 9.033, max = 12.657) and 17.374 (min = 13.332, max = 20.311) at the district level and 10.90 (min = 9.737, max = 12.978) and 17.41 (min = 15.134, max = 20.83) at the commune level for *S. fonquerniei* and *X. cheopis*, respectively (figure 3).

Variation in slope of the mean cumulative VDI was observable across species, communes and districts, and temperature treatments (uncorrected versus corrected); however, the degree of slope variation varies greatly (figure 4). There was a consistently greater variation in the VDI slope for *X. cheopis* (figure 4b,d,f,h) in comparison to *S. fonquerniei* (figure 4a,c,e,g). This was most obvious when comparing the two species across the same area (electronic supplementary material S1). Similarly, greater slope variation was observed under the uncorrected temperature treatment (figure 4a,b,e,f) than the corrected temperature treatment (figure 4c,d,g,h). Consequently, variation in slope was most clearly visible for *X. cheopis* under the uncorrected temperature treatment. For example, in Andrembesoa commune (high-altitude commune approx. 1200 m), there was a plateau in the VDI slope from May/June to October/November (figure 4f). The muted variation in VDI slope observed across the corrected temperature treatment (figure 4c,d,g,h) means that there are no clear periods of complete cessation in development, indicated by a plateau. However, the shallowest slope was generally concurrent with the May/June to October/November period, though it was difficult to confirm this across regions and treatments that show minimal slope variation, particularly for *S. fonquerniei*, under the corrected temperature treatment (figure 4c,g).

(c) Null models of vector development index slopes

The proportion of districts or communes where the VDI slope preceding a human plague case was significantly steeper than expected from the null distribution was much higher for the uncorrected temperature treatment (61.8–14.7%, figure 5a,c,e,g) compared to the corrected treatment (13–5.9%, figure 5b,d,f,h). Generally, the proportion of slopes significantly steeper than the null distributions were highest under the 1 month gradient period and decreased as the gradient period was increased over 2, 3 and 6 months.

There were 34 districts that reported human plague cases across the 2014–2020 period (figure 5a,b,c,d) and 75 communes across the 2018–2020 period (figure 5e,f,g,h). We would expect 5% of the *p*-values across both administrative areas to be significant due to chance. This equates to 2 (1.7) and 4 (3.75) for districts and communes, respectively. For the uncorrected temperature treatment, many more districts (5–21 districts or 14.7–61.8% of all districts) and communes (18–43 communes or 24–57.3% of all communes) were observed to have VDI slopes preceding human plague cases that were significantly steeper than expected from the null distribution. The values were much lower for the corrected temperature treatment, with fewer districts (2–4 districts or 5.9–11.8% of all districts) and communes (5–10 communes or 6.7–13% of all communes) showing

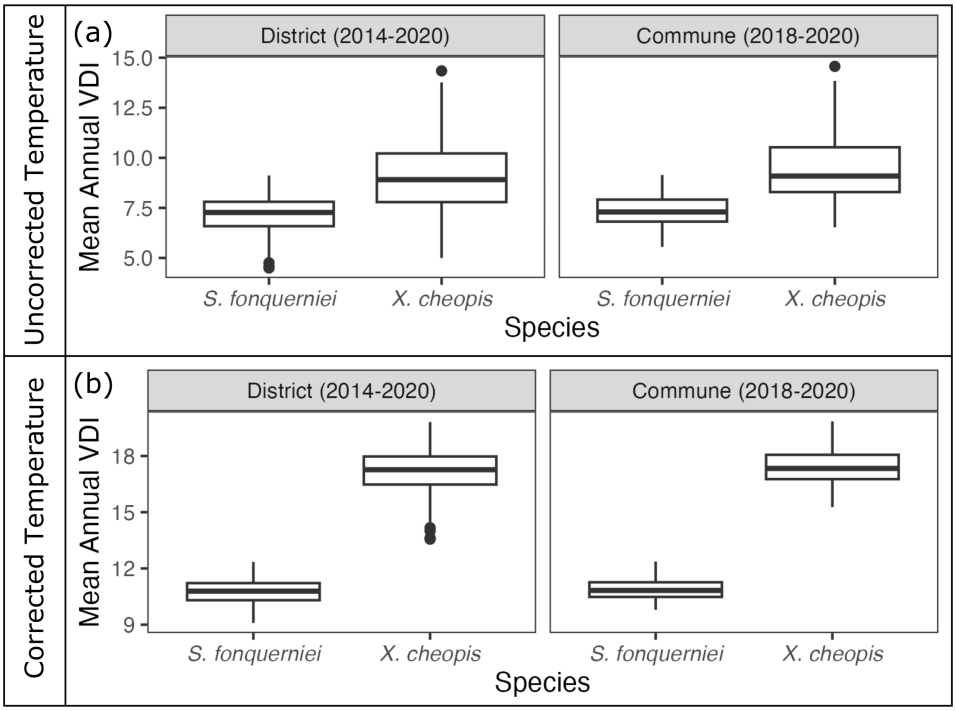

Figure 3. Mean annual VDI across all administrative areas of the Central Highlands of Madagascar. Plots for both uncorrected (a) and corrected (b) temperatures are shown. District (second administrative level) VDI data are displayed over the 2014–2020 period and commune data (third administrative level) over the 2018–2020 period. This division follows the availability of human plague case data across the highlands, and VDI has therefore been calculated following these divisions.

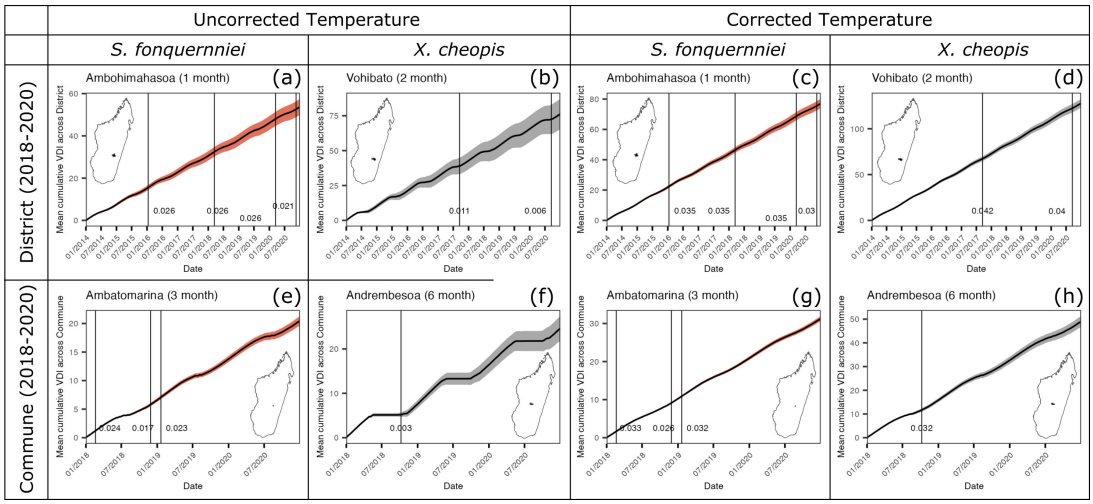

Figure 4. Examples of the VDI slope plots showing the timing of human plague cases (vertical lines) for four administrative areas across the Central Highlands of Madagascar (a, b, c and d are districts, e, f, g and h are communes), with the slope calculated across the range of periods prior to reported human plague cases (1, 2, 3, 6 months, stated in titles). Slopes are presented for the uncorrected (a, b, c and f) and corrected (c, d, g and h) temperatures. The text represents the calculated VDI slope prior to the human plague case. The line represents the mean VDI across the area, and the shaded ribbon (terracotta: *S. fonquerniei*, grey: *X. cheopis*) represents the SD in VDI across each area. The inset maps show the location of the selected district or commune. VDI slope plots for the remainder of the areas are in electronic supplementary material S1.

significance. The values across the corrected temperature treatment are closer to, although still slightly higher than, the expected significance due to chance. *S. fonquerniei* showed a consistently greater proportion of significant areas in comparison to *X. cheopis* for the uncorrected, but not for the corrected, treatment.

4. Discussion

Our results were partially consistent with the hypothesis that climatically mediated vector development was a key contributor to the initiation of the human plague season in the Central Highlands of Madagascar. However, the findings must be caveated by the greatly diminished consistency with the hypothesis observed when a temperature correction, based on short-term field validation, was applied to our model. Through this short-term field validation, we found that the *microclimf* model consistently

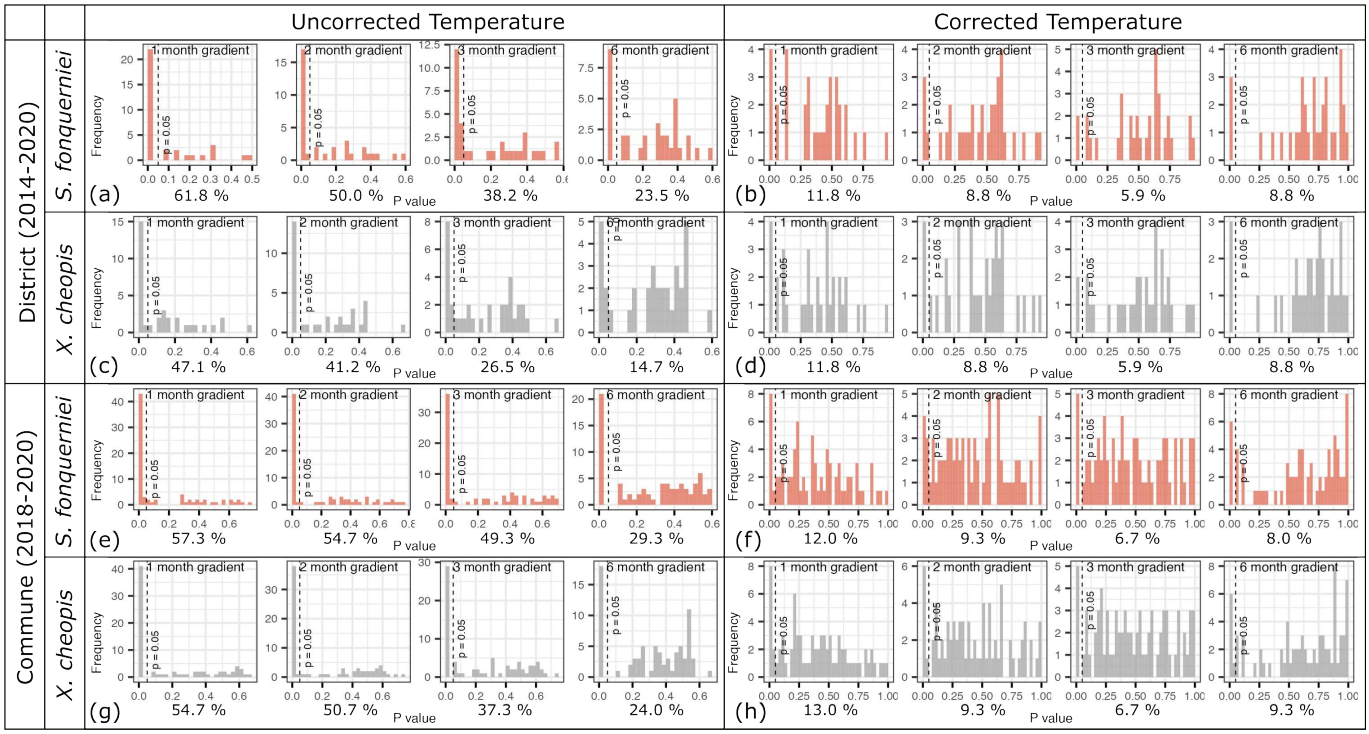

Figure 5. Significance of pre-plague case VDI slopes when compared to null cases across all districts (a, b, c and d) and communes (e, f, g and f) across the Central Highlands of Madagascar. The terracotta plots represent *p*-values of the comparisons of VDI with the null values for *S. fonquerniei* (a and b), and the grey plots represent *X. cheopis* (c and d). Plots are presented for the uncorrected (a, c, e and g) and corrected (b, d, f and h) temperatures. The dashed line indicates the 0.05 significance level; values to the left of this show that VDI slopes prior to human plague cases were significantly higher than those for the null cases. The percentage below each plot shows the percentage of districts or communes in which the VDI slope preceding a plague case was significantly higher than the null (1 decimal place).

underpredicted below-ground microclimate temperatures across the Central Highlands, and to a lesser degree, above ground at low heights (electronic supplementary material, text S1–S3). Confirming the microclimate within burrows was key to our understanding of this system, as the uncorrected temperature analysis was consistent with our hypothesis. However, once the temperatures had been corrected in line with the field validation, there was only minor seasonal variation in VDI.

The temperature treatment considered had the largest single impact on determining whether districts and communes exhibited a significantly higher VDI slope prior to recorded human plague cases than our nulls (i.e. vector development rates prior to human plague cases were not significantly greater than prior to null time points). The uncorrected temperature results (figures 3a, 4a,b,e,f, 5a,c,e,g) were generally consistent with the hypothesis that climatically mediated vector development was influencing human infection. Annual slope variation differs between area and species, with *X. cheopis* in high-altitude (colder) areas showing the greatest slope variation (e.g. figure 4f). The timing of this variation was consistent with the cool winter period (May/June and October/November), showing the lowest VDI slopes. This low period of VDI slope matches well with the observed low-plague season, from April to September [11]. The greatest proportion of areas with significantly higher VDI slopes prior to human plague cases was across the 1 month gradient period (47.1–61.8%), decreasing as the gradient period increased to 6 months (14.7–29.3%). This suggests that, if climate-mediated vector development was indeed influencing human plague infection, the mechanism linking climate to plague infection functions rapidly and was hence most observable over a 1 month time scale. Although this work suggests that vector development was a key part of this mechanism, we do not capture several other potentially co-incident factors such as flea activity and transmission of *Y. pestis*, both of which are impacted by microclimate and hence warrant further investigation [44–46]. The combined influence of climate and vector development was much less consistent across the corrected temperature model, in which all temperatures were increased by +6.03°C, based on brief (24 h) field validation. This increase in temperature works to reduce the variation in VDI slope, as there were very limited periods where both species were outside of their thermal development window. Under the corrected temperature treatment, several districts and communes exhibited a significantly higher VDI slope prior to recorded human plague cases than our nulls; however, this occurred much less frequently than under the uncorrected temperature treatment (5.9–13.0%). When considering the hypothesis that climate-mediated vector development influenced human plague cases, the two temperature treatments showed different levels of consistency, underscoring the need to investigate burrow microclimates and their role in vector development more closely.

Earlier studies revealed that flea development rates were highly correlated with temperature and relative humidity, although in some species, relative humidity had a weaker relationship if certain humidity thresholds had been achieved [47,48]. Humidity has not been observed to impact development times of the two species investigated here, although it may increase mortality in *S. fonquerniei* [24]. We therefore expected temperature to be the primary factor that mediated vector development and thus contributed to the peak in *S. fonquerniei* abundance at the beginning of the human plague season [7,49]. Given the experimental evidence that revealed the development of the two investigated species was not strongly influenced by humidity and that host

burrow humidity was maintained at a stable high humidity (67.5–100%), it is unlikely that humidity is a development-limiting factor in this system either (electronic supplementary material, figure S4) [24].

There are several biotic factors not captured by our model that may influence pre-imaginal development, such as intra- and interspecies competition for food resources among pre-imaginal fleas within the burrow. Flea larvae commonly feed on organic debris within the burrow, which ranges from host (rodent) and flea faeces to flea eggs, younger larvae and naked pupae [41]. However, such specific competition was rarely observed in the highlands, with rodents sampled within houses mostly infected with *X. cheopis*, whereas *S. fonquerniei* was commonly found in agricultural and forest areas [16]. This suggests that in the pre-imaginal phases, species rarely share the same burrows, thereby limiting the potential for within-burrow interspecies competition. To validate this, further sampling of the burrow systems is required to identify the flea species during the pre-imaginal phases.

The differing thermal development thresholds between *S. fonquerniei* and *X. cheopis* (9°C and 12.5°C, respectively) have been hypothesized as a key factor in explaining the limited distribution of *S. fonquerniei* and subsequently *Y. pestis* below 800 m [24]. At higher and cooler altitudes across the Central Highlands, *S. fonquerniei* and *X. cheopis* are both present; however, they exploit differing niches, with *X. cheopis* restricted to warmer indoor locations, while *S. fonquerniei* is present across rural and agricultural settings [24]. This difference in niche used by the two species makes it hard to determine the impact of competition. Compared to *X. cheopis*, *S. fonquerniei* fleas demonstrate higher transmission efficiency of *Y. pestis*, which may contribute to the distribution of the bacteria across Madagascar. Our modelling suggested that within the burrow environments in the Central Highlands, temperatures rarely drop below the development threshold for *S. fonquerniei*, as can be seen by variation in VDI slopes throughout our investigation periods (figure 4b,f). Furthermore, there was only a minor difference in the mean annual VDI completed between species, despite the longer development period for *S. fonquerniei*. We did not, however, attempt to model or sample microclimates within houses; therefore, despite our model suggesting that the Central Highland climate may favour the development rate of *S. fonquerniei*, further work is required to determine whether any competition occurs between these two vector species.

This study aimed to determine whether a pathway existed between climate, vectors and disease incidence without the need to integrate the dynamics of host species. The assumption is that the host species are not involved in the pre-imaginal development of the vectors, as this occurs off-host; hence, the vectors and the bacterium can operate independently of hosts. This is similar to the plague niche hypothesis, which posits that the distribution of *Y. pestis* is not simply a patchwork of possible host distributions but has a distribution independent of host species [50]. However, *R. rattus* abundances in the Central Highlands have recently been observed to be highly seasonal with peak abundances observed in June to August (dry season) [10,16,51]. Further, their distribution is likely to be seasonal, driven by both climate and, given their commensality, agricultural practices [52,53]. These factors may then suggest that the host species does, in fact, have an impact on pre-imaginal development of vectors, possibly through their metabolic impact on burrow environments, or larval stages consuming organic matter produced by hosts [41]. The climatic dynamics of host species may partially explain the geographically limited positive findings reported here. This suggests that vector and host dynamics, as well as the impact of external factors such as agricultural harvesting and storage, all impact zoonotic transmission of *Y. pestis*. It is possible that there is a stronger relationship between VDI and plague infection in rodents, but unfortunately, data relating to *Y. pestis* infection in rodents are currently unavailable to enhance our models. Human cases represent only spillover events, while transmission within rodent populations should be more directly linked to vector abundance. Efforts should be made to further understand and model the movement ecology and behaviour of host species, not just *R. rattus*, but other potentially important reservoir (introduced and endemic) species across this area [7,51,54].

5. Conclusion

Our findings contribute to a more nuanced understanding of the role of microclimate in shaping *Y. pestis* vector dynamics in the Central Highlands of Madagascar. This study provides evidence that microclimatic variation, particularly as represented by our uncorrected temperature treatment, can influence *Y. pestis* vector development and, in turn, plague case timing in Madagascar's Central Highlands. The uncorrected temperature outputs showed markedly higher proportions of locations where vector development rates preceding human plague cases were significantly elevated compared with the null expectation, whereas the corrected temperature treatment reduced this pattern substantially. This discrepancy highlights the sensitivity of modelled outcomes to assumptions about burrow temperatures and highlights the need for long-term monitoring of rodent burrow microclimates across representative habitats. The findings from this work will contribute to the development of future methods for modelling *Y. pestis* dynamics across varied landscapes and timeframes. Future work should integrate burrow microclimate measurements with concurrent trapping of host species, quantification of flea populations and pathogen detection. By combining these datasets within mechanistic frameworks, it will be possible to disentangle interactions in the climate–vector–host–pathogen system and improve predictions of high-risk locations and time periods. Such knowledge could enhance plague surveillance, guide targeted interventions and ultimately contribute to reducing *Y. pestis* persistence in endemic landscapes.

Ethics. This work did not require ethical approval from a human subject or animal welfare committee.

Data accessibility. The meteorological and environmental data for construction of the microclimate model are all freely available. Sample code, data (including dummy human plague data) and an explanatory readme are uploaded to Dryad [55]. The human plague data analysed in

this study are curated by the Plague Unit of the Institut Pasteur de Madagascar. These data can be made available upon reasonable request to peste@pasteur.mg.

Supplementary material is available online [56].

Declaration of AI use. We have not used AI-assisted technologies in creating this article.

Authors' contributions. H.G.F.: conceptualization, data curation, formal analysis, investigation, methodology, project administration, validation, visualization, writing—original draft, writing—review and editing; J.B.: writing—review and editing; F.R.: investigation, writing—review and editing; B.R.: investigation, writing—review and editing; L.S.: investigation, writing—review and editing; M.J.: conceptualization, funding acquisition, methodology, project administration, resources, software, writing—review and editing; V.A.: writing—review and editing; K.K.: methodology, writing—review and editing; N.C.S.: writing—review and editing; I.M.D.M.: methodology, software, writing—review and editing; M.R.: investigation, writing—review and editing; A.C.A.: conceptualization, formal analysis, funding acquisition, investigation, methodology, supervision, writing—review and editing; S.A.: conceptualization, funding acquisition, investigation, project administration, supervision, writing—review and editing.

All authors gave final approval for publication and agreed to be held accountable for the work performed therein.

Conflict of interest declaration. We declare we have no competing interests.

Funding. This work was funded by Natural Environment Research Council (NE/W00321X/1). N.C.S. was funded by an ERC Synergy grant (Synergy-Plague, reference number ERC-2023-SyG, GA no. 101118880).

Acknowledgements. We would like to thank the technical team at the University of Nottingham School of Geography, Teresa Needham, Jodie Brown and John Corr, for equipment and fieldwork preparations. Further, we would like to thank Haingotiana Rakoto-Ramambason from the Ministry of Health Madagascar (Health and Environment Division) and Mamy Gabriel from the Ministry of Public Health (Plague Division) for invaluable help in the field. We would further like to thank IPM administrative and technical staff for support throughout the project.

References

1. Stenseth NC, Atshabar BB, Begon M, Belmain SR, Bertherat E, Carniel E, Gage KL, Leirs H, Rahalison L. 2008 Plague: past, present, and future. *PLoS Med.* **5**, e3. (doi:10.1371/journal.pmed.0050003)
2. Schrag SJ, Wiener P. 1995 Emerging infectious disease: what are the relative roles of ecology and evolution? *Trends Ecol. Evol.* **10**, 319–324. (doi:10.1016/s0169-5347(00)89118-1)
3. Bertherat E. 2016 Plague around the world, 2010–2015/La peste a travers le monde: 2010–2015. *Weekly Epidemiol. Record* **91**, 89–94.
4. Chanteau S, Ratsifasoamanana L, Rasoamanana B, Rahalison L, Randriambelosoa J, Roux J, Rabeson D. 1998 Plague, a reemerging disease in Madagascar. *Emerg. Infect. Dis.* **4**, 101–104. (doi:10.3201/eid0401.980114)
5. Alderson J, Quastel M, Wilson E, Bellamy D. 2020 Factors influencing the re-emergence of plague in Madagascar. *Emerg. Top. Life Sci.* **4**, 423. (doi:10.1042/ETLS20200334)
6. Randremanana R *et al*. 2019 Epidemiological characteristics of an urban plague epidemic in Madagascar, August–November, 2017: an outbreak report. *Lancet Infect. Dis.* **19**, 537–545. (doi:10.1016/s1473-3099(18)30730-8)
7. Rasoamalala F *et al*. 2024 Population dynamics of plague vector fleas in an endemic focus: implications for plague surveillance. *J. Med. Entomol.* **61**, 201–211. (doi:10.1093/jme/tjad152)
8. Laperrière V, Brugger K, Rubel F. 2016 Cross-scale modeling of a vector-borne disease, from the individual to the metapopulation: the seasonal dynamics of sylvatic plague in Kazakhstan. *Ecol. Model.* **342**, 34–48. (doi:10.1016/j.ecolmodel.2016.09.023)
9. Brygoo E. 1966 Epidemiologie de la peste a Madagascar. *Med. Trop. (Mars)* **26**, 89–94.
10. Chanteau S *et al*. 2006 *Atlas de la peste à madagascar*. Paris, France: IRD Editions.
11. Andrianaivoarimanana V *et al*. 2019 Trends of human plague, Madagascar, 1998–2016. *Emerg. Infect. Dis.* **25**, 220–228. (doi:10.3201/eid2502.171974)
12. Kreppel KS, Caminade C, Telfer S, Rajerison M, Rahalison L, Morse A, Baylis M. 2014 A non-stationary relationship between global climate phenomena and human plague incidence in Madagascar. *PLoS Neglected Trop. Dis.* **8**, e3155. (doi:10.1371/journal.pntd.0003155)
13. Migliani R, Chanteau S, Rahalison L, Ratsitorahina M, Boutin JP, Ratsifasoamanana L, Roux J. 2006 Epidemiological trends for human plague in Madagascar during the second half of the 20th century: a survey of 20,900 notified cases. *Trop. Med. Int. Health* **11**, 1228–1237. (doi:10.1111/j.1365-3156.2006.01677.x)
14. Rahelinirina S, Rajerison M, Telfer S, Savin C, Carniel E, Duplantier JM. 2017 The Asian house shrew *Suncus murinus* as a reservoir and source of human outbreaks of plague in Madagascar. *PLoS Neglected Trop. Dis.* **11**, e0006072. (doi:10.1371/journal.pntd.0006072)
15. Rahalison L *et al*. 2004 Susceptibility to Plague of the Rodents in Antananarivo, Madagascar. In *The Genus Yersinia. Advances in Experimental Medicine and Biology* (eds M Skurnik, JA Bengoechea, K Granfors), pp. 439–442, vol. **529**. Boston, MA: Springer. (doi:10.1007/0-306-48416-1_87)
16. Andrianaivoarimanana V, Kreppel K, Elissa N, Duplantier JM, Carniel E, Rajerison M, Jambou R. 2013 Understanding the persistence of plague foci in Madagascar. *PLoS Neglected Trop. Dis.* **7**, e2382. (doi:10.1371/journal.pntd.0002382)
17. Barbieri R, Signoli M, Chevé D, Costedoat C, Tzortzis S, Aboudharam G, Raoult D, Drancourt M. 2020 Yersinia pestis: the natural history of Plague. *Clin. Microbiol. Rev.* **34**, e00044-19. (doi:10.1128/CMR.00044-19)
18. Stenseth NC *et al*. 2006 Plague dynamics are driven by climate variation. *Proc. Natl Acad. Sci. USA* **103**, 13110–13115. (doi:10.1073/pnas.0602447103)
19. Ben-Ari T, Gershunov A, Tristan R, Cazelles B, Gage K, Stenseth NC, Ben-Ari T. 2010 Interannual variability of human plague occurrence in the Western United States explained by Tropical and North Pacific Ocean climate variability. *Am. J. Trop. Med. Hyg.* **83**, 624–632. (doi:10.4269/ajtmh.2010.09-0775)
20. Kemppinen J *et al*. 2024 Microclimate, an important part of ecology and biogeography. *Glob. Ecol. Biogeogr.* **33**, e13834. (doi:10.1111/geb.13834)
21. Samuel MD, Poje JE, Rocke TE, Metzger ME. 2022 Potential effects of environmental conditions on prairie dog flea development and implications for sylvatic plague epizootics. *EcoHealth* **19**, 365–377. (doi:10.1007/s10393-022-01615-6)
22. Pauling CD, Finke DL, Anderson DM. 2021 Interrelationship of soil moisture and temperature to sylvatic plague cycle among prairie dogs in the Western United States. *Integr. Zool.* **16**, 852–867. (doi:10.1111/1749-4877.12567)
23. Kearney MR, Enriquez-Urzelai U. 2023 A general framework for jointly modelling thermal and hydric constraints on developing eggs. *Methods Ecol. Evol.* **14**, 583–595. (doi:10.1111/2041-210x.14018)
24. Kreppel KS, Telfer S, Rajerison M, Morse A, Baylis M. 2016 Effect of temperature and relative humidity on the development times and survival of *Synopsyllus fonquerniei* and *Xenopsylla cheopis*, the flea vectors of plague in Madagascar. *Parasit. Vectors* **9**, 1–10. (doi:10.1186/s13071-016-1366-z)

25. Kreppel K. 2012 The effect of climate on the epidemiology of plague in Madagascar. PhD thesis, University of Liverpool. https://livrepository.liverpool.ac.uk/id/eprint/3174073.
26. Sharif M. 1949 Effects of constant temperature and humidity on the development of the larvae and the pupae of the three Indian species of *Xenopsylla* (Insecta: Siphonaptera). *Phil. Trans. R. Soc. Lond. B* **233**, 581–633. (doi:10.1098/rstb.1949.0004)
27. Fell HG, Osborne OG, Jones MD, Atkinson S, Tarr S, Keddie SH, Algar AC. 2022 Biotic factors limit the invasion of the plague pathogen (*Yersinia pestis*) in novel geographical settings. *Glob. Ecol. Biogeogr.* **31**, 672–684. (doi:10.1111/geb.13453)
28. Lembrechts JJ *et al*. 2020 SoilTemp: a global database of near-surface temperature. *Glob. Chang. Biol.* **26**, 6616–6629. (doi:10.1111/gcb.15123)
29. Wild J, Kopecký M, Macek M, Šanda M, Jankovec J, Haase T. 2019 Climate at ecologically relevant scales: a new temperature and soil moisture logger for long-term microclimate measurement. *Agric. For. Meteorol.* **268**, 40–47. (doi:10.1016/j.agrformet.2018.12.018)
30. Kearney MR, Porter WP. 2017 NicheMapR – an R package for biophysical modelling: the microclimate model. *Ecography* **40**, 664–674. (doi:10.1111/ecog.02360)
31. Maclean IMD, Mosedale JR, Bennie JJ. 2019 Microclima: an R package for modelling meso- and microclimate. *Methods Ecol. Evol.* **10**, 280–290. (doi:10.1111/2041-210x.13093)
32. Haider N, Kirkeby C, Kristensen B, Kjær LJ, Sørensen JH, Bødker R. 2017 Microclimatic temperatures increase the potential for vector-borne disease transmission in the Scandinavian climate. *Sci. Rep.* **7**, 8175. (doi:10.1038/s41598-017-08514-9)
33. Maclean IMD, Klinges DH. 2021 Microclimc: a mechanistic model of above, below and within-canopy microclimate. *Ecol. Model.* **451**, 109567. (doi:10.1016/j.ecolmodel.2021.109567)
34. Kolstela J *et al*. 2024 Revealing fine-scale variability in boreal forest temperatures using a mechanistic microclimate model. *Agric. For. Meteorol.* **350**, 109995. (doi:10.1016/j.agrformet.2024.109995)
35. Hersbach H *et al*. 2020 The ERA5 global reanalysis. *Q. J. R. Meteorol. Soc.* **146**, 1999–2049. (doi:10.1002/qj.3803)
36. Friedl MA, Sulla-Menashe D, Tan B, Schneider A, Ramankutty N, Sibley A, Huang X. 2010 MODIS collection 5 global land cover: algorithm refinements and characterization of new datasets. *Remote Sens. Environ.* **114**, 168–182. (doi:10.1016/j.rse.2009.08.016)
37. Hengl T *et al*. 2021 African soil properties and nutrients mapped at 30 m spatial resolution using two-scale ensemble machine learning. *Sci. Rep.* **11**, 6130. (doi:10.1038/s41598-021-85639-y)
38. Kafle P, Peller P, Massolo A, Hoberg E, Leclerc LM, Tomaselli M, Kutz S. 2020 Range expansion of muskox lungworms track rapid arctic warming: implications for geographic colonization under climate forcing. *Sci. Rep.* **10**, 17323. (doi:10.1038/s41598-020-74358-5)
39. Snyder RL, Spano D, Cesaraccio C, Duce P. 1999 Determining degree-day thresholds from field observations. *Int. J. Biometeorol.* **42**, 177–182. (doi:10.1007/s004840050102)
40. World Health Organization. 2006 International meeting on preventing and controlling plague: the old calamity still has a future. *Weekly Epidemiol. Record* **81**, 278–284.
41. Krasnov BR. 2008 *Functional and evolutionary ecology of fleas: a model for ecological parasitology*. Cambridge, UK: Cambridge University Press. (doi:10.1017/CBO9780511542688)
42. Ruxton GD, Neuhäuser M, O'Hara RB. 2013 Improving the reporting of P-values generated by randomization methods. *Methods Ecol. Evol* **4**, 1033–1036. (doi:10.1111/2041-210X.12102)
43. Maclean IMD *et al*. 2021 On the measurement of microclimate. *Methods Ecol. Evol.* **12**, 1397–1410. (doi:10.1111/2041-210X.13627)
44. Schotthoefer AM *et al*. 2011 Effects of temperature on the transmission of *Yersinia pestis* by the flea, *Xenopsylla cheopis*, in the late phase period. *Parasites Vectors* **4**, 191. (doi:10.1186/1756-3305-4-191)
45. Beugnet F, Chalvet-Monfray K, Loukos H. 2009 FleaTickRisk: a meteorological model developed to monitor and predict the activity and density of three tick species and the cat flea in Europe. *Geospat. Health* **4**, 97–113. (doi:10.4081/gh.2009.213)
46. Self S, Yang Y, Walden H, Yabsley MJ, McMahan C, Herrin BH. 2024 A nowcast model to predict outdoor flea activity in real time for the contiguous United States. *Parasites Vectors* **17**, 27. (doi:10.1186/s13071-023-06112-5)
47. Krasnov BR, Khokhlova IS, Fielden LJ, Burdelova NV. 2001 Development rates of two *Xenopsylla* flea species in relation to air temperature and humidity. *Med. Vet. Entomol.* **15**, 249–258. (doi:10.1046/j.0269-283x.2001.00295.x)
48. Silverman J, Rust MK, Reierson DA. 1981 Influence of temperature and humidity on survival and development of the cat flea, *Ctenocephalides felis* (Siphonaptera: Pulicidae). *J. Med. Entomol.* **18**, 78–83. (doi:10.1093/jmedent/18.1.78)
49. Klein J, Uilenberg G. 1966 Données faunistiques et écologiques sur les puces de Madagascar (Siphonaptera). *Cahiers ORSTOM Entomologie Médicale* **4**, 31–60.
50. Maher SP, Ellis C, Gage KL, Enscore RE, Peterson AT. 2010 Range-wide determinants of plague distribution in North America. *Am. J. Trop. Med. Hyg.* **83**, 736–742. (doi:10.4269/ajtmh.2010.10-0042)
51. Parany MNJ *et al*. 2026 Plague in small mammals from an endemic focus of the malagasy central highlands: a longitudinal survey with a special reference on black rats (*Rattus rattus*). *Integr. Zool.* **21**, 37–47. (doi:10.1111/1749-4877.12944)
52. McCauley DJ *et al*. 2015 Effects of land use on plague (*Yersinia pestis*) activity in rodents in Tanzania. *Am. J. Trop. Med. Hyg.* **92**, 776–783. (doi:10.4269/ajtmh.14-0504)
53. Mulungu LS, Ngowo V, Mdangi M, Katakweba AS, Tesha P, Mrosso FP, Mchomvu M, Sheyo PM, Kilonzo BS. 2013 Population dynamics and breeding patterns of multimammate mouse, *Mastomys natalensis* (Smith 1834), in irrigated rice fields in eastern Tanzania. *Pest Manag. Sci.* **69**, 371–377. (doi:10.1002/ps.3346)
54. Mahmoudi A *et al*. 2020 Plague reservoir species throughout the world. *Integr. Zool.* **16**, 820–833. (doi:10.1111/1749-4877.12511)
55. Fell H, Bailey J, Rasoamalala F *et al*. 2026 Data and code from: Integrating microclimate to understand vector development and disease patterns: Challenges and lessons from plague in Madagascar's Central Highlands. [Dataset]. Dryad Digital Repository. (doi:10.5061/dryad.p2ngf1w32)
56. Fell HG *et al*. 2026 Supplementary material from: Integrating microclimate to understand vector development and disease patterns: challenges and lessons from plague in Madagascar's Central Highlands. Figshare. (doi:10.6084/m9.figshare.c.8335608)